This manuscript was published as formal in:

***Carbohydrate Polymers* 2017, 165, 39-50**

DOI: 10.1016/j.carbpol.2017.02.027

https://doi.org/10.1016/j.carbpol.2017.02.027

***Title*:**

Salicyl-imine-chitosan hydrogels. Supramolecular architecturing as a crosslinking method toward multifunctional hydrogels

Manuela-Maria Iftime, Simona Morariu, Luminita Marin*

lmarin@icmpp.ro

”Petru Poni” Institute of Macromolecular Chemistry of Romanian Academy – 41A, Aleea Gr. Ghica Voda, Iasi, Romania

ABSTRACT

Hydrogels based on chitosan and salicyladehyde were obtained by dynamic covalent chemistry. The unusual chitosan gelling in the presence of the monoaldehyde has been deciphered following and correlating data of NMR, FTIR, single crystal and wide angle XRD, POM and optical measurements. Of significant importance in understanding the crosslinking features was the synthesis of a model compound and the successfully growth as single crystal allowing the study of its supramolecular peculiarities. The hydrogels exhibited in SEM a porous or fibrous morphology, in good correlation with the crosslinking degree. They swelled very fast, similar to the superporous hydrogels of third generation and exhibited self-healing properties. Rheological investigation demonstrated good mechanical properties, thermosensitivity and thixotropy. The paper revealed a hydrogel with suitable properties for use in bio-medical applications, and moreover, revealed a new concept of obtaining chitosan hydrogels using monoaldehydes – which are widespread in nature, cheap and beneficial to the human body.

Keywords: chitosan; dynamic covalent chemistry; superporous; luminescence; thixotropy; self-healing

INTRODUCTION

1. Hydrogels are a class of materials applied in many fields of human life, especially in those bio-related: substrates for biomedical engineering and pharmacology, environment protection, agriculture, food industry, hygiene and so on [Ahmed, 2015; Caló, & Khutoryanskiy. 2015; Shen, Shamshina, Berton, Gurau & Rogers, 2016]. Advances in hydrogel domain intersected the modern domain of supramolecular chemistry, moving from static to dynamic complexity in hydrogel design. Dynamic (hydro)gels were prepared based on reversible reactions, of physical or chemical nature: acylhydrazone bonds [Deng, Tang, Li., Jiang & Chen, 2010], Schiff bases [Zhang, Tao, Li & Wei, 2011], reversible ring-opening of 1,2 dithiolanes [Barcan, Zhang & Waymouth, 2015], boronic ester transesterification [Brooks & Sumerlin, 2016], thiol–disulphide interconversion [Casuso et al., 2015], metalophilic attractions [Casuso et al., 2014], metal–ligand exchange [Sreenivasachary, & Lehn, 2005] or telechelic dendritic macromolecules with multiple adhesive termini [Wang et al., 2010]. The use of reversible connections for crosslinking led to a new generation of smart materials/hydrogels able to respond to environmental stimuli or artificial triggers. They usually exhibit self-healing behaviour and have the capability to recover quickly their mechanical properties after removing the stress.

2. Among various reversible covalent connections used for obtaining dynamic materials, the condensation of amino groups with carbonyl functionalities to yield imines also known as Schiff bases or azomethines is considered the most powerful strategy used in dynamic covalent chemistry to generate structures of high complexity, dynamic nanoarchitectures and materials with modulable properties [Liu & Lim, 2013; Roy, Bruchmannb & Lehn, 2015] or in dynamic combinatorial chemistry to trigger the easy selection of components as response to external physical stimuli or chemical effectors [Sreenivasachary & Lehn, 2005; Zhang & Barboiu, 2016; Clima, Peptanariu, Pinteala, Salic & Barboiu, 2015; Turin-Moleavin, 2015]. The advantages of reversible imine linkage consist mainly in its fast exchange tuned by the reagent reactivity, the presence of water, the pH or the temperature. Moreover, the equilibrium of the imine exchange is an active intermediate/target in many biological processes and pharmaceutical chemistry as enzyme catalysis [Fisher & Viswanathan, 1984], signaling through G-protein-coupled receptors [Perez & Karnik, 2005], transamination, obtaining of biomarkers or reaction of sugars with biological relevant amines [Qin, Long, Panunzio & Biondi, 2013]. From these reasons, the reversible imine connection is of great interest in chemistry, biology and materials science and was implemented for the search of biologically active substances [Roy, Bruchmannb & Lehn, 2015; Zhang & Barboiu, 2016; Clima, Peptanariu, Pinteala, Salic & Barboiu, 2015; Turin-Moleavin, 2015; Ramstrom, Lohmann, Bunyapaiboonsri & Lehn, 2004; Marin et al., 2016; Nasr et al., 2009].

3. In this context, preparation of dynamic chitosan hydrogels based on reversible imine connections appears as a promising and challenging design. Chitosan is a naturally derived, biocompatible polymer which already proved high applicability in biochemistry and bioengineering [Bhattarai, Gunn & Zhang, 2010; Delmar, & Bianco-Peled, 2016; Nawrotek, Tylman, Rudnicka, Balcerzak & Kamiński, 2016; Giri et al., 2012]. Some previous preliminary studies of our group noticed the possibility of chitosan gelling with some monoaldehydes [Marin, Simionescu & Barboiu 2012; Marin et al., 2015], by a dynamic process of physico-chemical crosslinking [Ailincai et al., 2016; Marin et al., 2014]. The topic is of high interest taking into consideration that monoaldehydes exist in a large variety, many of them being natural products with therapeutic properties, compared to the dialdehydes which are generally used for chitosan crosslinking which were proved to have a toxicity degree [Beauchamp et al., 1992; Berger et al., 2004; Mikhailov et al., 2016]. Thus, hydrogels obtained from natural products as chitosan and natural aldehydes should have better premises for safer bio-related applications. Herein, we explored the obtaining of hydrogels based on the natural products, chitosan and salicylaldehyde, in order to provide a hydrogel appropriate for bio-applications, and to pave a way of chitosan crosslinking by a new friendly method. Salicylaldehyde has been chosen as possible chitosan crosslinker due to its intrinsic properties. Natural occurring in buckwheat seeds, exudate from castor sacs or larval defence secretions of several beetle species, salicylaldehyde was approved by the U.S. Food and Drug Administration (FDA) and Flavour and Extract Manufacturers Association (FEMA) [Adams, et al., 2005; Salicylaldehyde, 1979] for food use. It was demonstrated that it has antifungal, anti-mycotoxigenic and chemosensitizing properties and is evaluated in the chemotherapy of invasive fungal diseases and in agriculture as inhibitor of fungal growth and mycotoxin production [Kim, Campbell, Mahoney, Chan, & Molyneux, 2011]. Moreover, studies on its imine derivatives proved antimicrobial and antifungal properties [da Silva et al.,

2011; Zaltariov et al. 2015; de Araújo, Barbosa, Dockal, & Cavalheiro, 2017] and even anti-cancer features [Garrick et al., 1991].

4. Two aspects must be highlighted here: (i) chitosan gelling with monoaldehydes is a new topic in the chitosan chemistry which development was started by us; (ii) even if a few papers reported the obtaining and the properties of imine derivatives based on chitosan and salicylaldehyde [e.g. de Araújo, Barbosa, Dockal, & Cavalheiro, 2017; Menaka, & Subhashini, 2016; Deng, Fei, & Feng, Y. 2011; dos Santosa, Dockala & Cavalheiro, 2005], there are no studies in literature dedicated to the salicyl-imine-chitosan hydrogels, neither on their formation or their properties. The study reported here reveals in fact a novel hydrogel with good mechanical properties, thermosensitivity, thixotropy, self-healing, fast swelling, and luminescence keeping the promise for bio-applications.

5.

EXPERIMENTAL SECTION

Materials

Low molecular weight chitosan (263 kDa) with a degree of deacetylation (DA) of 83 %, salicylaldehyde 98 %, D-glucosamine hydrochloride 99 %, ethanol, glacial acetic acid and phosphate buffer solution of pH 7.4 were purchased from Sigma–Aldrich Co. (USA) and were used as received. The number of the free amino groups of chitosan was calculated on the basis of DA. Acetate buffer solution of pH 4.2 was prepared as described by Lambert and Muir [Lambert & Muir, 1973]. Bidistilled water was obtained in the laboratory.

Synthesis of the model compound: 2((o-hydroxybenzylidene)amino)-5-(hydroxymethyl) tetrahydro-1H-pyran-1,3,4-triol (MC)

D-glucosamine hydrochloride, (0.3 g, 1.39 mmol) was suspended in methanol (4.41 ml) with 1 equiv. of finely grinded solid NaOH (0.058 g, 1.39 mmol). After 5 minute, the resulted NaCl was filtered off. Salicylaldehyde (0.043 ml, 1.39 mmol) was slowly added to the filtrate,

and the reaction mixture was kept at ~35^{o}C, up to a yellow solid precipitated, after 5 minutes. The mixture was cooled in an ice bath; the solid was filtered off, washed with ice-cold methanol and dried under vacuum for 2 days [Nguyen, Nguyen, Ho, & Ngo, 2011; Costa Pessoa, Tomaz & Henriques, 2003]. The yellow powder was recrystallized from ethanol to give yellow needles single crystals with a yield of ~10%.

Single crystal of **MC** was mounted in inert oil and transferred to the cold gas stream of the diffractometer. Structure determination of crystal data: $C_{13}H_{17}NO_5$: M_r= 267 g mol^{-1}; space group I2; cell lengths: a=13.1519(8) Å b=6.0602(2) Å, c=17.1108(11) Å; cell angles: α=90 ^{o}, β=105.219(6) ^{o}, γ=90 ^{o}; cell volume V=1315.96 Å^3. The right structure has been confirmed by FTIR, ^{1}H-NMR and ^{13}C-NMR spectra, too (Figure 1s, 2s).

Preparation of the hydrogels and xerogels

The synthesis of the hydrogels was carried out by acid condensation reaction of the chitosan with salicylaldeyde. Briefly, a 1% solution (g mL^{-1}) of salicylaldehyde in ethanol (Table 1) was added drop wise to a 2 % solution (g mL^{-1}) of chitosan (0.3 g, 1.473 mmol glucosamine repeating units) in acidic water (0.7 % acetic acid solution: 105 μL of acetic acid in 15 mL of water), under vigorous magnetic stirring (750 rpm), at 50 ^{o}C. The molar ratio between the NH_2 and CHO functional groups has been varied, keeping constant the amount of chitosan and changing the amount of aldehyde to achieve hydrogels with different crosslinking densities (Table 1). The hydrogels appeared as transparent yellowish semisolid materials with smooth texture, without air bubbles or other macroscopic particles, as also Cavalheiro noticed [de Araújo, Barbosa, Dockal, & Cavalheiro, 2017]. The visual formation of hydrogels was observed after 8 minutes in the case of 1/1 molar ratio of the NH_2/CHO functional groups (**S1**), after 3 hours in the case of 1.5/1 (**S1.5**) and of 2/1 (**S2**) respectively, and after 1 week in the case of 2.5/1 (**S2.5**). For a lower amount of aldehyde (NH_2/CHO=3/1 (**S3**); 3.5/1(**S3.5**)) the reaction medium transformed into a viscous liquid which still flew even after 2 weeks. All hydrogels

were kept uncovered for two days up to the initial volume of chitosan solution was reached. According to the NMR analysis which indicated the increase of the conversion of the amine groups into imine linkages during 16 days, the hydrogels were further kept covered another two weeks for gelling maturation. The corresponding xerogels of the obtained hydrogels were prepared by lyophilization. A 2 % chitosan solution in 0.7 % acetic acid has been also lyophilized, to be used as reference (**S0**). The xerogels weight was similar with that of the initial reagents, indicating no mass loss during lyophilization.

Table 1. The reaction parameters and codes of the studied hydrogels

Code	**So**	**S1**	**S1.5**	**S2**	**S2.5**	**S3**	**S3.5**	**S4**
NH_2/CHO ratio	1:0	1:1	1.5:1	2:1	2.5:1	3:1	3.5:1	4:1
Chitosan (g mol^{-1})	0.3/ 1.473	0.3/ 1.473	0.3/ 1.473	0.3/ 1.473	0.3/ 1.473	0.3/ 1.473	0.3/ 1.473	0.3/ 1.473
SA (g mol^{-1})	-	0.180/ 1.473	0.120/ 0.982	0.090/ 0.736	0.07/ 0.589	0.06/ 0.491	0.0514/ 0.421	0.0450/ 0.368
Ethanol (mL)	-	18	12	9	7	6	5.14	4.5
Xerogel (g)	0.3	0.48	0.42	0.39	0.37	0.36	0.35	0.34

SA: salycilaldehyde

Methods

In order to analyse the structure and morphology of the hydrogels, the corresponding xerogels were obtained by freezing in liquid nitrogen and further submitted to lyophilization using a LABCONCO FreeZone Freeze Dry System equipment, for 24 hours, at -54 ºC and 1.510 mbar.

FTIR spectra of the xerogels were registered using a FT-IR Bruker Vertex 70 Spectrofotometer, by ATR technique and processed using Origin8 software.

The NMR spectra were obtained on a Bruker Avance DRX 400 MHz Spectrometer equipped with a 5 mm QNP direct detection probe and z-gradients. In the case of hydrogels, the chemical shifts were reported as δ values (ppm) relative to the residual peak of the

deuterated water used as solvent. In the case of the model compound, the chemical shifts were reported as δ values (ppm) relative to the residual peak of the DMSO-d_6 used as solvent.

Crystallographic measurements of the model compound (**MC**) were performed with an Oxford-Diffraction XCALIBUR E CCD diffractometer equipped with graphite-monochromated Mo Kα radiation. The single crystal was positioned at 40 mm from the detector and 460 frames were measured each for 30 s over 1° scan width. The unit cell determination and data integration were carried out using the CrysAlis package of Oxford Diffraction [CrysAlis RED, 2003]. The structure was solved by direct methods using Olex2 software [Dolomanov, Bourhis, Gildea, Howard & Puschmann, 2009] with the SHELXS structure solution program and refined by full-matrix least-squares on F^2 with SHELXL-97 [Sheldrick, 2008]. Atomic displacements for non-hydrogen atoms were refined using an anisotropic model. Hydrogen atoms have been placed in fixed, idealized positions accounting for the hybridization of the supporting atoms and the possible presence of hydrogen bonds in the case of donor atoms. The molecular plots were obtained using the Olex2 program.

Wide angle X-ray diffraction (WXRD) of the xerogel pellets was performed on a Bruker D8 Avance diffractometer with the Ni-filtered Cu-Ka radiation (l = 0.1541 nm), in the range of 2-40° (2 theta). The working conditions were 36 kV and 30 mA and data were handled by the FullProf 2000 program. The xerogel pellets were obtained in a manual Hydraulic Press, by applying a pressure of 10 N m^{-1}. The d-spacing corresponding to each reflection band was calculated applying the Bragg low $2d\sin\theta = n\lambda$, where λ is the wavelength of the X-ray emitted by the copper source (0.1541 nm) and n=1. It was considered that the planes giving rise to the smallest Bragg angle have the largest d-spacing attributed to the interlayer distance according to the single crystal X-ray diffraction of the model compound.

Polarized light microscopy observations were performed by using an Olympus BH-2 polarized light microscope. The optical observations were performed on thin slices of hydrogel placed between two clean untreated glass slides.

The xerogel morphology was studied with a field emission Scanning Electron Microscope SEM EDAX – Quanta 200 at accelerated electron energy of 15 or 20 KeV.

The rheological investigations were carried out by using a MCR 302 Anton-Paar rheometer equipped with a Peltier device. A plane-plane geometry (diameter of 50 mm) and an anti-evaporation device which limits the water evaporation were used. The first rheological test performed on each investigated sample consisted in stress amplitude sweep in order to establish their linear viscoelastic regime. The oscillatory and continuous shear measurements were performed at 37 °C in the frequencies (ω) range of 0.1 – 100 rad s^{-1} and in the range of shear rate ($\dot{\gamma}$) from 10^{-3} s^{-1} to 10^{2} s^{-1}. The loss modulus (G''), the storage modulus (G'), and the complex viscosity (η^*) were determined by the oscillatory deformation tests. In addition, the zero shear viscosity (η_o) and the critical yield stress (τ_o) were established by the continuous shear tests. The thixotropic recovery of the samples was investigated by following the apparent viscosity as a function of time when a stepwise sequence of 0.2 s^{-1} – 10 s^{-1} – 0.2 s^{-1} was applied. The first and second steps were set at 100 s and the third step was about 150 s when the equilibrium was reached. The oscillatory measurements were also carried out at different temperatures from the range 20 °C - 40 °C in order to establish the effect of temperature on the viscoelastic properties of the investigated hydrogels.

For swelling measurements, the xerogels were cut in square-shape and dried under vacuum overnight. Three samples of each xerogel were weighed and then introduced into sealed vials containing 15 mL of distilled water or buffer solution. Then, the xerogel samples were weighted at different time intervals, following their taking off from solution and their surface blotting on a filter paper up to constant weight. The mass equilibrium swelling (MES) was

calculated according to the equation MES = $(M_s-M_d)/M_d$, where M_s is the weight of the swollen hydrogel and M_d the weight of the hydrogel in the dried state. Data presented in this experiment were the mean values of triplicate measurements.

RESULTS AND DISCUSSION

Supramolecular hydrogels with superporous morphology were obtained by reacting chitosan with salicylaldehyde in specific conditions (Scheme 1). As the crosslinking of chitosan with a monoaldehyde is an unusual pathway of hydrogel obtaining, in order to explore the driving forces that governed their forming, FTIR, ^{1}H-NMR and X-ray diffraction measurements were investigated in detail. To confirm the chemical pathway and supramolecular peculiarities employed in their forming, a model compound (**MC**) was synthesized from glucosamine (chitosamine) and salicylaldehyde (Scheme 1s) and successfully grown as single crystals.

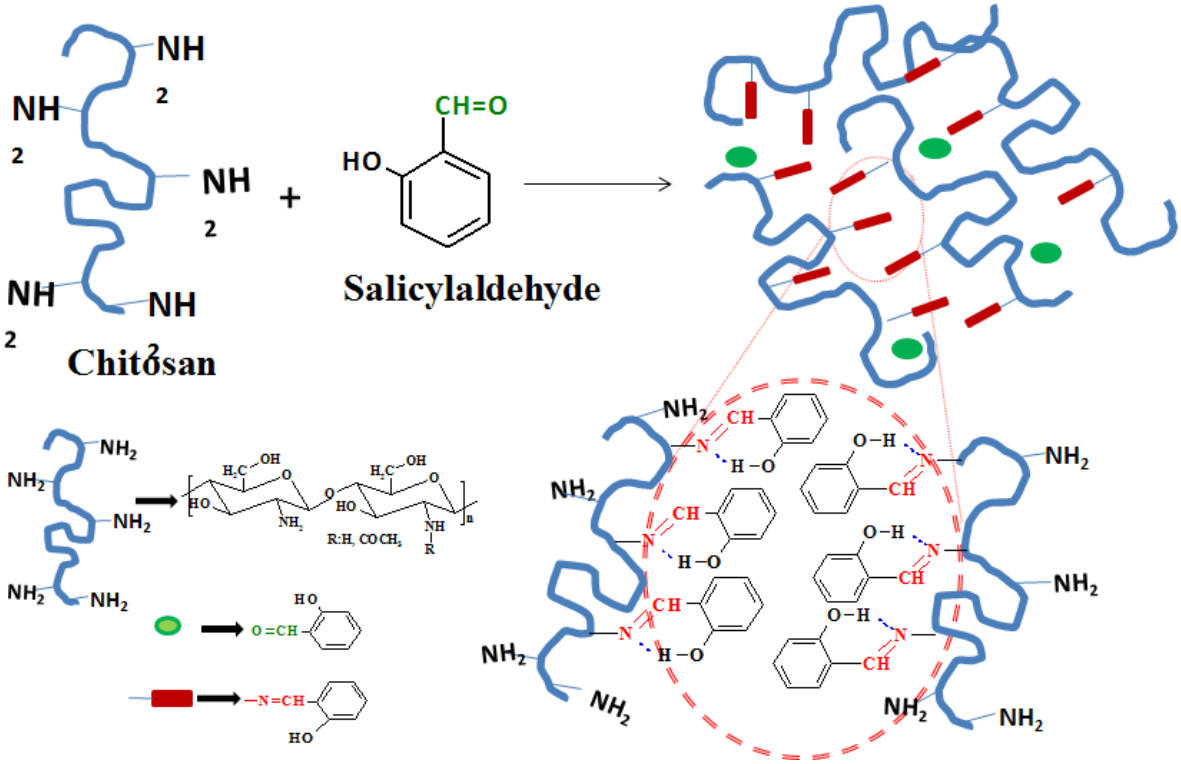

Scheme 1. Synthesis of the salicyl-imine-chitosan hydrogels

NMR spectroscopy

The structural characterization by NMR spectroscopy of the model compound evidenced the forming of the covalent imine linkage by the presence of the chemical shift of its proton as two bands at 8.49 and 8.42 ppm due to the α and β conformers formed in solution (Figure 1s) [Costa Pessoa, Tomaz & Henriques, 2003; Destri, Khotina & Porzio, 1991]. Compared to the model compound, the hydrogels showed the chemical shift of the imine proton as a single band, consistent with the stabilization of the imine linkage *via* an "imine clip" effect by the formation of an intramolecular H-bond between the imine nitrogen and the neighboring OH group [Kovaricek, & Lehn, 2012], characteristic to the solid state (Figure 1a) [Filarowski, 2005; Marin, van der Lee, Shova, Arvinte, & Barboiu, 2015]. Another feature of the hydrogel NMR spectra is the presence of the chemical shift of the aldehyde proton, indicating the incomplete conversion of the aldehyde groups into imine units, due to the reversibility of the imine forming in water [Kovaricek, & Lehn, 2012; Sagiomo, & Luning, 2009]. The monitoring of the aldehyde conversion into imine units by measuring the C<u>H</u>=N/C<u>H</u>O integral ratio exhibited that the reaction equilibrium was continuously shifted to the products during 16 days, when became constant (Figure 1b). This evolution of the integral ratio together with the stabilization of the imine units by intramolecular H-bonding characteristic to the solid state, indicated the forming of "out-of-solution" imine units [Marin et al., 2014], possible by the formation of hydrophobic clusters by the self-organization of the newly formed imine rigid units (Scheme 1).

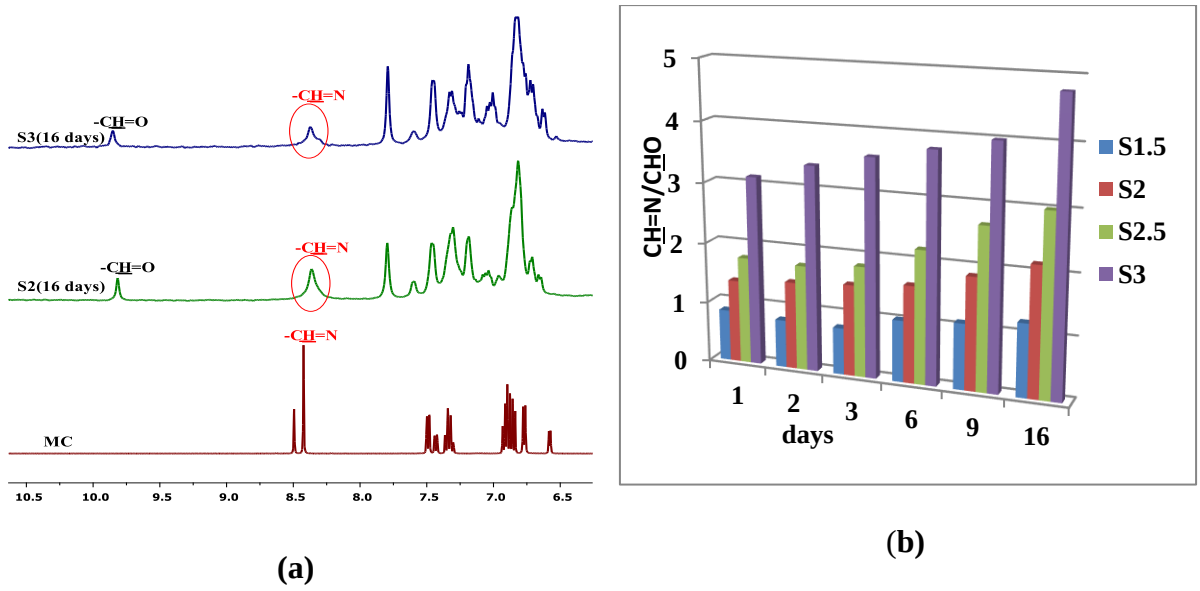

(a) **(b)**

Figure 1. (a) NMR spectra of the model compound and representative hydrogels; (b) graphic representation of the evolution of the CH=N/CHO integral ratio over time

FTIR spectroscopy

The FTIR spectrum of the **MC** shows an intense sharp band at 1631 cm^{-1} corresponding to the group stretching vibration of the imine linkage [Marin, van der Lee, Shova, Arvinte & Barboiu, 2015] and an intense broad band centred at 3393 cm^{-1} attributed to the preponderant intermolecular H-bonds rising between O-H…O pyranosic rings (see Supramolecular arrangement section) [Kumirska et al., 2010]. The FTIR spectra of the xerogels presented significant changes compared to that of the chitosan parent but were quite similar to the **MC** one, indicating similar chemical transformations and packaging peculiarities (Figure 2). Thus, in the xerogel FTIR spectra, the characteristic imine band appeared as a sharp peak at 1632 cm^{-1}, confirming the covalent bonding of the salicylaldehyde to the chitosan chain *via* imine linkage [dos Santosa, Dockala & Cavalheiro, 2005]. Oppositely to the NMR investigation, no evidence of some unreacted aldehyde could be seen in the FTIR spectra, the characteristic vibration band of the aldehyde group at 1670 cm^{-1} was absent. As no aldehyde was lost during the lyophilization process, the absence of the aldehyde in the FTIR spectra of the xerogels was

attributed to the complete shifting of the reaction equilibrium to the products during the water removing [Sagiomo & Luning, 2009]. The imine band was more intense as the content of salicylaldehyde was higher and significant more intense compared to the band of the amide group of chitosan at 1645 cm^{-1} which appeared only as a weak shoulder, highlighting the higher density of the imine units on the chitosan chain compared to the amide ones. The increasing of the intensity of the imine band was accompanied by the diminishing of the amine band (vibration of the N-H linkage at 1550 cm^{-1}), once again confirming the conversion of the amine functional groups into imine linkages during the condensation reaction. Comparing NMR and FTIR data it could be estimated that during the hydrogel freezing, the free water formed crystals, while the chitosan, water H-bonded, non-reacted aldehyde and ethanol and acetic acid traces were concentrated in a non-frozen liquid where the condensation reaction continued, process well documented in the case of the cryogel preparation [Dinu, Ozmen, Dragan & Okay, 2007].

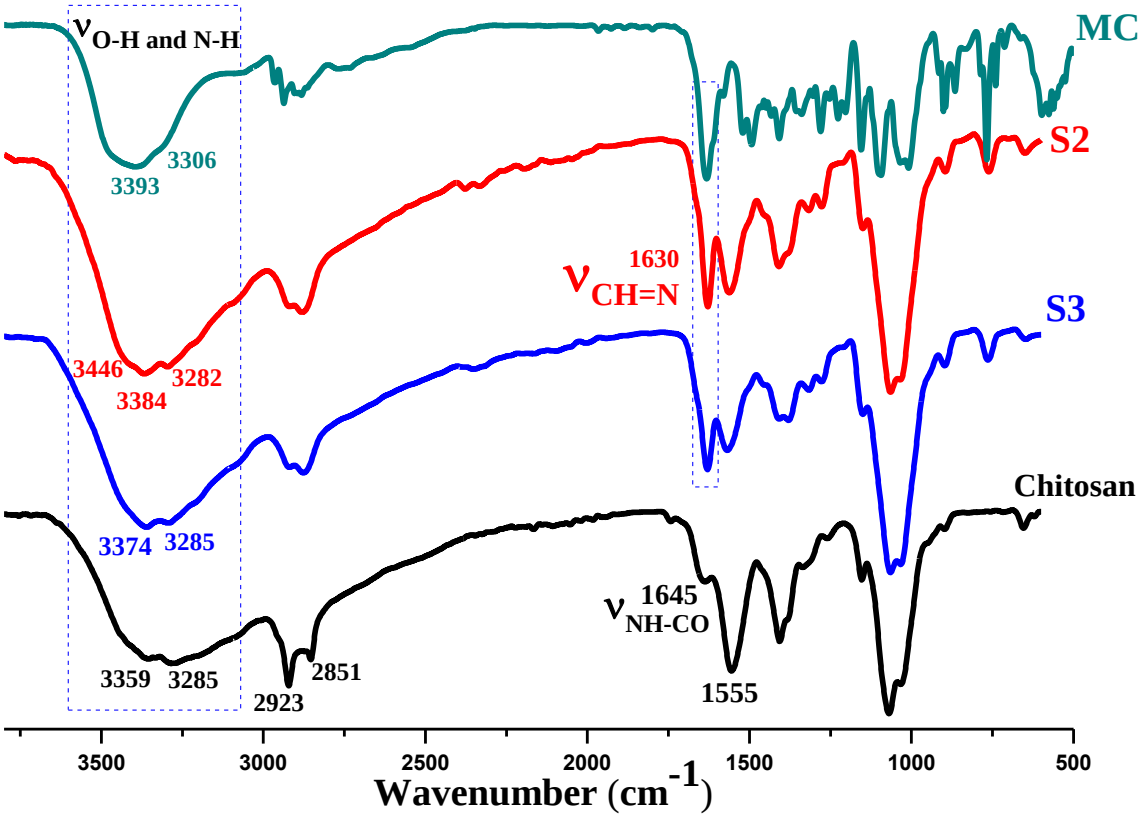

Figure 2. FTIR spectra of the chitosan, model compound and representative xerogels

Important changes in the FTIR spectra could be seen in the 3500-2800 cm^{-1} region related to the OH stretching vibration, intra- or intermolecular H-bonded. In this FTIR domain, chitosan presents mainly two superposed bands attributed to the –OH stretching vibration of the secondary OH at the C3 position intramolecular H-bonded to the O5 of an adjacent ring (3359 cm^{-1}) and to the primary OH in the C6 position involved in an inter-molecular H-bond with O3 atom of the neighbouring chain (3285 cm^{-1}). For the model compound, the superposed bands appeared shifted to higher wavenumbers (3393 and 3306 cm^{-1}, respectively) attributed to the tighter packing due to the presence of hydrophobic imine units which facilitated hydrophobic/hydrophilic segregation, and thus a redistribution of the H-bonds. Comparing the xerogel spectra with that of the chitosan parent and the model compound, it could be observed the change of this spectral domain depending by the aldehyde content. The gradually increasing

of the aldehyde content (**S3**; **S2.5**; **S2**) produced a gradually shifting of the superposed bands to the higher wavenumber (3374, 3285; 3385, 3292; and 3384, 3285 cm^{-1}), attributed by similarity with the model compound to the influence of the formation of the imine units inducing a tighter packing. Moreover, once the content of the aldehyde increased, a new peak at higher wavenumbers (3448 cm^{-1}) became more evident, especially in the case of **S1** (Figure 3s), suggesting the formation of new intermolecular H-bonds [Sun et al., 2008], in agreement with the WXRD measurements. This hypothesis is supported by the intensity modification of the stretching vibration bands of the C-H bonds in CH_2 group (2923 and 2851 cm^{-1}, respectively) indicating a rearrangement of H-bonding environment by grafting imine units on chitosan chains.

Supramolecular arrangement

The determination of the X-ray structure of the **MC** confirmed its expected molecular structure and gave valuable information related to the driving forces which guide the supramolecular interactions and crystal-packing in the solid state of such a system. As can be seen in Figure 3, the supramolecular arrangement of the model compound (**MC**) was dominated by the H-bonds generated by the presence of the hydroxyl groups.

Firstly, the imine linkage is stabilized through formation of an intramolecular hydrogen bond between the phenolic hydrogen and imine nitrogen (1.85 Å) giving an intramolecular 6-membered cycle which forced the imine to adopt a coplanar position with the aromatic ring (Figure 3a). The glucosamine ring exists in the typical chair conformation positioned in a trans-orientation to the aromatic ring, with respect to the C=N bond. The planes of the two rings (aromatic and pyranose) are in almost perpendicular position one to each other, with a torsion angle of 88.5 ^{o} (Figure 3b).

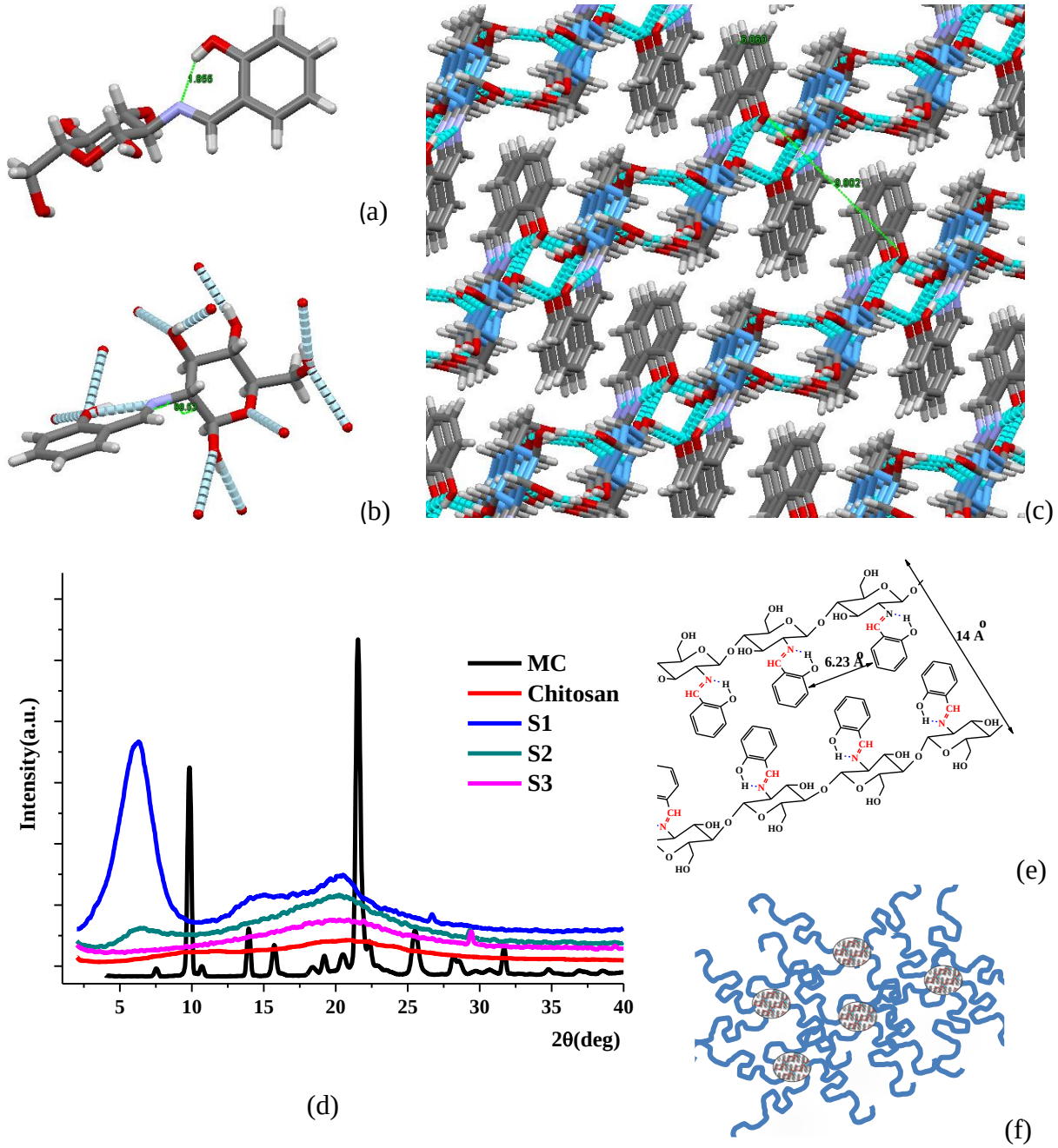

Figure 3. X-ray molecular structure of the **MC** in (a) 3D Print representation; (b) side view of the molecule with H-bonds and (c) view of its 3D supramolecular architecture in the crystal structure (for a better view of the hydrophobic/hydrophilic segregation, the pyranose ring has been represented in blue colour and the H-bonds in cyan); and (d) WXRD of the model compound and representative xerogels; (e) representation of the layering and d-spaces; (f) representation of the hydrogel network

Secondly, each pyranose ring is cofacial linked with two others through intermolecular O-H…..O H-bonds (1.9 Å) forming hydrophilic ribbons with opposite orientation (Figure 3c).

The neighbour ribbons are linked two by two *via* lateral intermolecular O-H…..O H-bonds resulting in the formation of hydrophilic layers. The phenolic -OH participates in the stabilization of the hydrophilic layers, through H-bonds and weak C-H…O type interactions (2.6 Å). On each hydrophilic layer, the hydrophobic aromatic imines lay sideway from, in orthogonal positions. The hydrophobic imine units belonging to vicinal hydrophilic layers are self-organized together forming hydrophobic layers. Thus, the **MC** has a hydrophilic-to-hydrophobic layered morphology which develops to a larger scale (Figure 3d).

The wide angle X-ray diffraction (WXRD) of the **MC** exhibited three main sharp reflection bands corresponding to the following d-spacing values, as calculated by Bragg law: (i) a band at 9.8 ^{o} corresponding to the inter-layer distance of 9 Å in agreement with the partial overlapping of the antiparallel alignment of the imine units within the hydrophobic layer thickness (Figure 3e); (ii) a band at 13.9 ^{o} corresponding to the intermolecular distance between two aromatic imine units of 6.4 Å in agreement with the intermolecular distance between aromatic rings or cofacial pyranosic rings, and (iii) a reflection band at 21.4 ^{o} corresponding to the intermolecular distance between two adjacent pyranose ribbons of about 4.2 Å. As can be seen the d-spacing values agree well with those given by the X-ray single crystal measurements.

The WXRD diffractograms of the xerogels revealed different profiles, in direct connection with the different density of the imine units. Thus, the xerogels with higher imine content (**S1**, **S1.5**, **S2**) have somehow a similar pattern to the **MC**, consisting in the presence of the three main reflections, corresponding to a three-dimensional ordering. However, their shape is broader – signature of the polydispersity of the d-spacing values imposed by the polymeric nature of the chitosan and the irregular grafting of the imine units. A distinctive feature of their WXRD pattern is given by the shifting of the reflection band from 9.8 ^{o} in the **MC** to a smaller angle of 6.3 ^{o} corresponding to a higher inter-layer distance of 14 Å. This is in agreement with the direct connection of the pyranosic rings of the chitosan chains with lower distance between

amine units, which hinders the overlapping of the imine units during the hydrophilic-hydrophobic segregation. The inter-layer distance of 14 Å agree well with the antiparallel ordering forming bilayers [Baron, 2001] of the imine units belonging to adjacent hydrophilic layers, as simulated by molecular mechanics MM+ method (Figure 3e).

The reflection bands corresponding to the intermolecular distance between the aromatic units and inter-ribbons distance, respectively, occurred around the same values as for **MC** (14 ^{o} and 20.4 ^{o}) indicating a similar motif of the arrangement of these building blocks; the inter-ribbons distance in **MC** corresponds to the inter-chain distance in xerogels. Compared to the WXRD pattern of the chitosan, the bands are sharper, of higher intensity, signature of the imine self-ordering in cybotactic groups [De Vries, 1970], forming hydrophobic clusters.

Oppositely, the xerogels with lower content of salicylaldehyde (**S2.5**, **S3**) exhibited a WXRD pattern closer as shape to that of the chitosan: the reflection band at lower angle misses and those at wider angle are of weak intensity – meaning that imine density was too low to assure their self-organization in a significant amount to form a layered structure. The exact position of the reflection bands, their intensity and the ratio of their intensities is given in the Table 1s.

Analysing the data of the three structural measurements (NMR, FTIR and XRD) and taking into consideration the under equimolar reaction conditions, the chitosan gelling in the presence of salicylaldehyde could be estimated as taking place due to a process of self-ordering. Mixing the chitosan and salicylaldehyde solutions, the self-assembling of salicylaldehyde and chitosan took place *via* an acid condensation reaction yielding imine units. The newly formed imine bonds were stabilized by intramolecular H-bonds forming rigid cores which tended to self-organize together. Further, due to the antagonistic character of the hydrophilic chitosan and hydrophobic imines, layered “out of water” hydrophilic-to-hydrophobic clusters were formed. They acted as net nodes for the chitosan chains and thus the gelling occurred. As a consequence

of the formation of the "out of water" clusters, the imination equilibrium shifted to the forming of new amounts of products (as NMR indicated), process which continued during the lyophilization. In the case of the equimolar ratio of the functional groups (**S1**), a layered morphology similar to a lamellar mesophase of lyotropic liquid crystals could be reached, while in the case of the under equimolar ratio (**S1.5-S3**) only "out of water" clusters formed linking the chitosan chains. The "out of water" clusters were of higher dimension with layered morphology in the case of **S1**, **S1.5**, **S2** hydrogels and of lower diameter for **S2.5**, **S3** hydrogels (see WXRD). Deeper studies on the reversible features of the salicyl-imine connection proved its high rate of formation and high rate of exchange giving, in appropriate conditions, intramolecular non-directional motional processes involving the transfer of the salicylaldehyde between amino functionalities by an aminal intermediate [Kovaricek & Lehn, 2012]. By similarity we estimated that the layered architecture of the "out of water" clusters was reached by intramolecular motions involving continuous exchange of the salicylaldehyde group between vicinal amine functionalities of chitosan. The "out of water" clusters created a protective environment of the imine units against water, enabling them to play the role of multibinder entities capable to crosslink the chitosan chains (Figure 3f). It is important to note the role played by the intramolecular H-bonds in the hydrogel formation. Comparing the ability of the chitosan gelling of salicylaldehyde containing the hydroxyl group in *ortho* position with that of other mono-aldehydes containing the hydroxyl group in *para* position (vanillin, *p*-hydroxy-benzaldehyde), it could be observed that the latest didn't promoted the hydrogel formation [Marin et al. 2015; Marin et al. 2013]. In these conditions, it is reasonable to affirm that the formation of the intramolecular H-bond favoured the gelling process by the formation of the rigid imine units which facilitated the self-organization in hydrophobic clusters.

The ordered nature of the hydrogels must be proved by a birefringent texture under polarized light microscopy. As can be seen in Figure 4a, the hydrogels showed a birefringent

streaky texture characteristic to the lyotropic liquid crystals. Moreover, a similar texture was observed for the **MC** model compound (Figure 4b) – demonstrated by single crystal X-ray diffraction to have a lamellar architecture. This similarity confirmed once again the supramolecular order of the hydrogels.

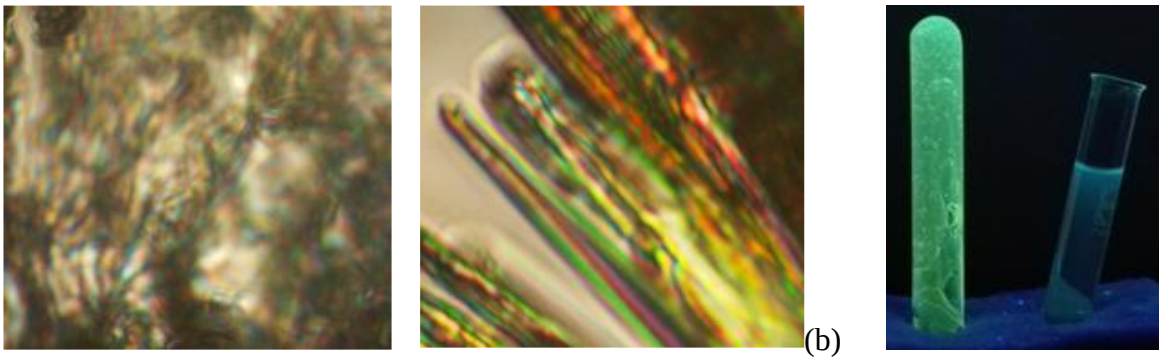

(a) (b) (c)

Figure 4. POM microphotographs of the (a) **S1** hydrogel and (b) **MC** model compound; and (c) hydrogel **S1** and **MC** solution under illumination with an UV lamp

On the other hand, the forming of the planar salycilimine units should result in chromophoric units which must emit light. As can be seen in Figure 4c, by illumination under an UV lamp, both the solution of the model compound and the hydrogels emitted light, confirming the extended conjugation of the rigid imine unit. However, while the **MC** solution (10^{-5} mol L^{-1}) emitted slight bluish light, the hydrogels emitted intense green light – signature of the layered periodic order into hydrogels giving structural colours [Zhang & Chen, 2015]. This is a challenging finding taking into consideration that fluorescent hydrogels are desirable soft materials for many bio-applications but their obtaining is complicated [Ma & Wang 2015].

Hydrogel morphology

SEM imaging of the xerogels has been used to qualitatively asses the microstructure of the hydrogels. As can be seen in Figure 5, the morphology of the hydrogels was dependent by the amount of salicylaldehyde used as crosslinker. For the highest amount – the morphology

consisted in interconnected pores with diameter around 100 μm (**S1**), while for the smallest amount – a fibrous network (**S3**) could be seen. The morphology of the other hydrogels with intermediate amount of aldehyde is heterogeneous consisting in a combination of pores and fibres connected together (**S1.5**, **S2**, **S2.5**). The rational explanation of this change of the morphology was given by the decreasing of the crosslinking density correlated with longer segments of "free" chitosan chains between the multibinder sites, capable of entrapping larger amounts of water.

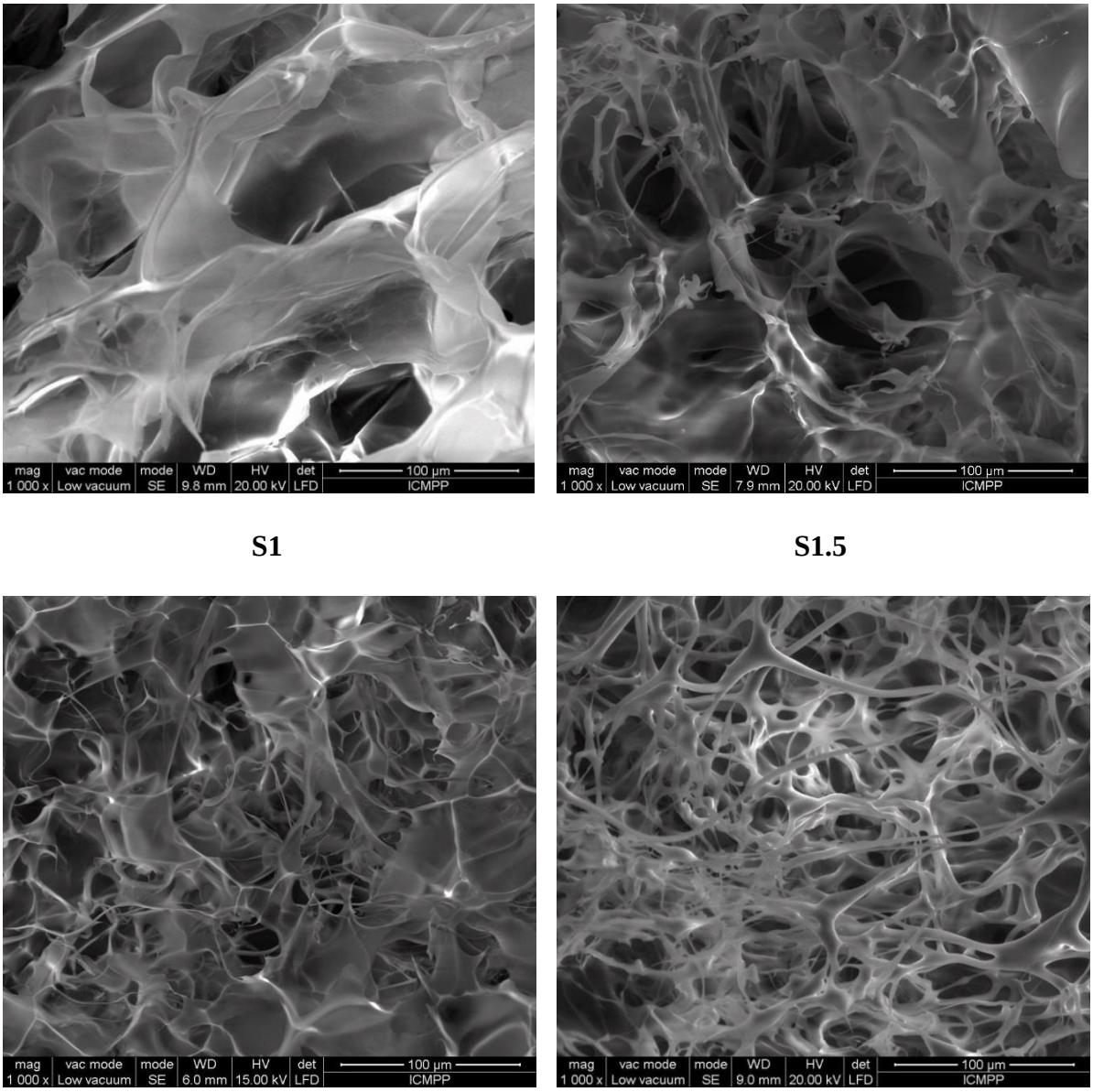

S1 **S1.5**

S2.5 **S3**

Figure 5. SEM microphotographs of the xerogels

Rheological properties

Hydrogels are soft materials with elastic properties, whose rheological features strongly influence their ability to be used in different bio-applications as drug delivery, wound dressing, artificial cartilage, or medical devices. Generally, the rheological properties of the hydrogels based on chitosan strongly depend on the preparation method [Morariu, Bercea & Brunchi, 2015; Bercea, Bibire, Morariu, Teodorescu & Carja, 2015].

To establish the physical state of the **S1**-**S3.5** samples and the minimum amount of salicylaldehyde necessary for sol-gel transition, the elastic and storage moduli were determined. The gel-like behaviour associated with an elastic modulus higher than viscous one ($G' > G"$) occurred for the **S1.5**-**S3** samples (Figure 6a, Table 2s). The elastic modulus at 1 rad·s^{-1} increased by increasing the aldehyde content from 0.543 Pa for **S3** to 265 Pa for **S1.5**, corresponding to an increasing of the stiffness of the crosslinked network.

Applying the Chambon and Winter method which considers that $tan\ \delta$ is independent of the frequency at the gel point [Chambon & Winter, 1987], the NH_2/CHO ratio corresponding to the sol-gel transition has been found at 3.3 (Figure 6b).

The apparent viscosity (η) of the investigated samples, measured in continuous shear rate, revealed high values at low shear rate for the hydrogels obtained in the presence of a higher salicylaldehyde amount, related to the higher density of the multibinder sites. The value of the apparent viscosity decreased step wise with about an order of magnitude for each hydrogel, according to the easier destruction of the multibinder entities with lower ordering degree.

All the understudy hydrogels showed a pseudoplastic (shear-thinning) behaviour characterized by the decrease of η with increasing the shear rate ($\dot{\gamma}$) (Figure 6c). It could be appreciated that chain closeness facilitated new inter- and intra-chain H-bonding in the gel structure, but at higher share rates, the repulsions between similarly charged sites became

predominant and disrupted the networking architecture. Under shear stress, η kept a constant value (η_o) up to a critical yield stress (τ_o), when abruptly decreased in the case of gel-like samples, corresponding to the starting point of the hydrogel flow (Figure 6d). As can be seen in the inset of Figure 6d, the start of the hydrogel flowing depended on the amount of salicylaldehyde. The threshold values of the τ_o of the hydrogels gradually increased as the salicyladehyde content increased, in agreement with their stiffer and stronger structure due to the higher density of the multibinder sites and their larger size. The η_o and τ_o values of the studied samples are given in Table 2s.

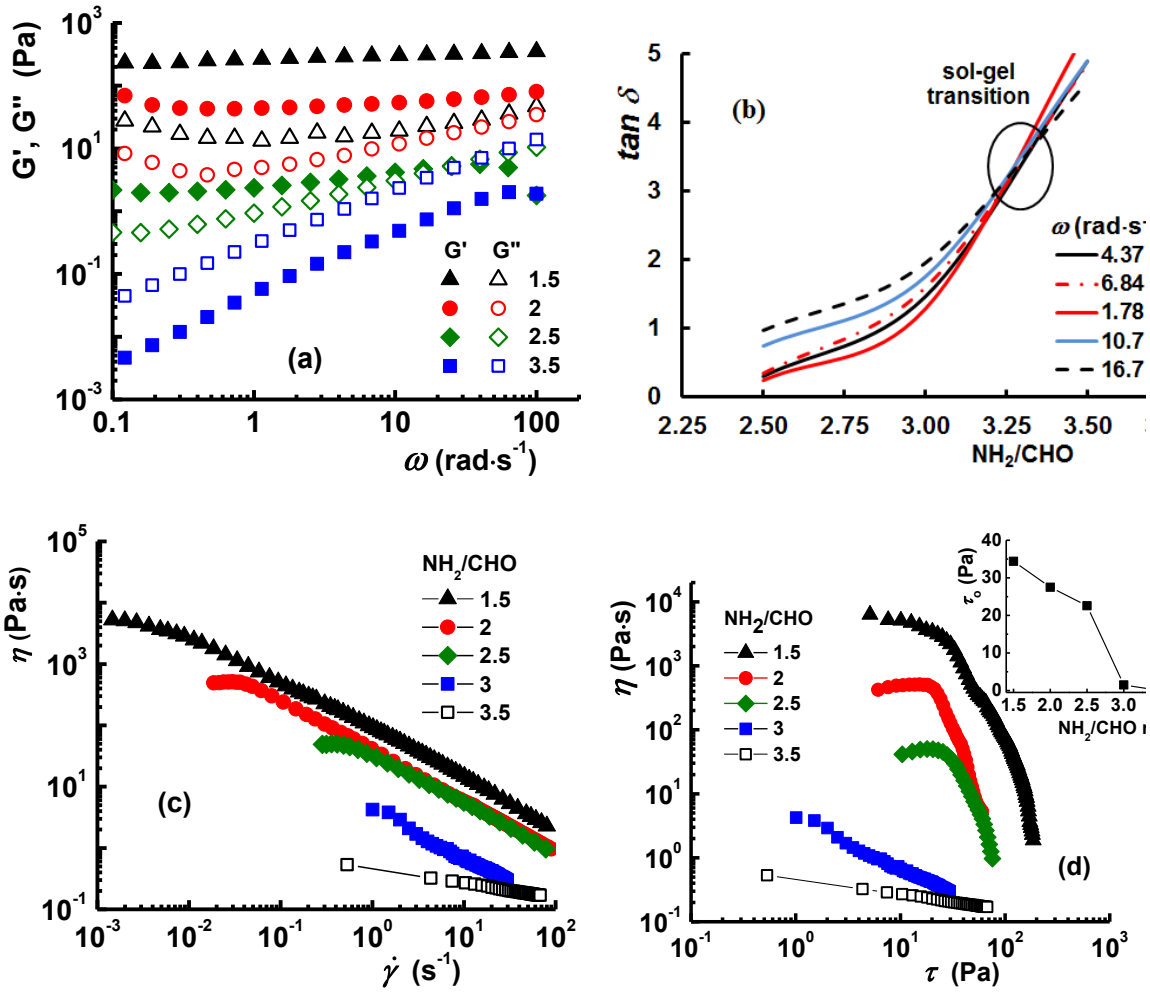

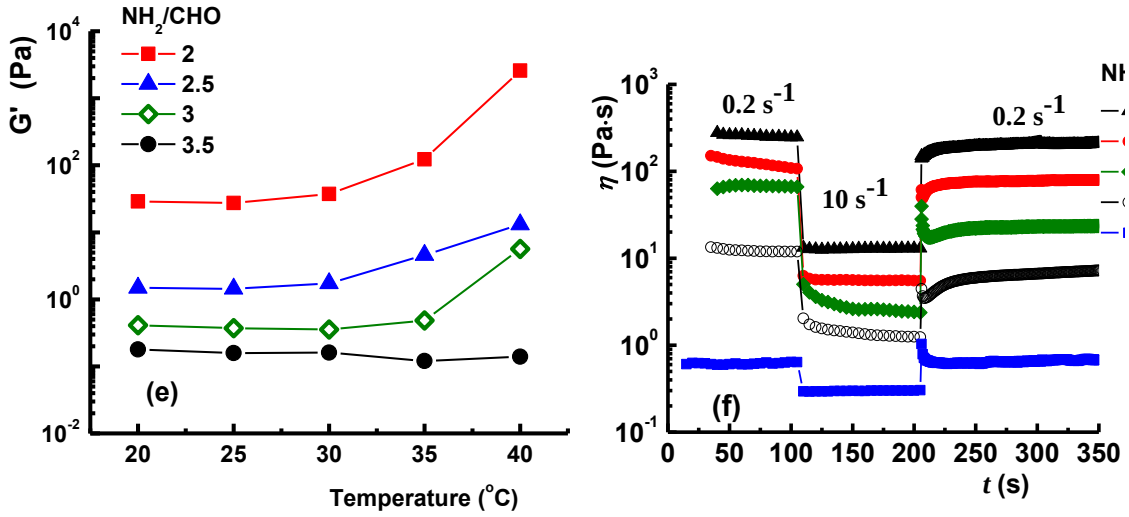

Figure 6. Rheological investigations: (a) Dependence of *G'* and *G"* on the oscillatory frequency (ω); (b) loss tangent ($tan\ \delta = G"/G'$) at various frequencies on the NH_2/CHO ratio, at 37 °C; Apparent viscosity *versus* (c) shear rate and (d) shear stress, at 37 °C (Inset figure represents the variation of yield stress as a function of NH_2/CHO ratio); (e) Effect of the temperature on elastic modulus at 0.3 rad·s^{-1} and (f) apparent viscosity as a function of time obtained using a shear rate stepwise procedure (0.2 s^{-1} – 10 s^{-1} – 0.2 s^{-1})

The temperature sweep tests revealed that the viscoelastic moduli of the hydrogels (**S2-S3**) were independent on the temperature up to 30 °C. The further heating determined the increase of the viscoelastic moduli of the hydrogels with higher content of salicylaldehyde proving thermosensitivity (Figure 6e). The thermosensitivity has been explained by the shifting of the carbonyl/imine equilibrium to the products at higher temperature which favoured the formation of the "out of water" clusters increasing by this the crosslinking density, expressed by the rise of elastic modulus. The viscoelastic parameters of **S2-S3.5** samples, determined at different temperatures and 0.3 rad·s^{-1}, are shown in Table 3s.

Variation of the apparent viscosity as a function of time when a stepwise sequence of 0.2 s^{-1} - 10 s^{-1} - 0.2 s^{-1} is applied can give clues about the thixotropy of the samples (Figure 6f). In the first step, when a shear rate of 0.2 s^{-1} was applied, all samples, excepting **S2**, exhibited a constant apparent viscosity during 100 s. When the shear rate was increased at 10 s^{-1}, the

apparent viscosity of all samples decreased indicating a shear-thinning behaviour. **S2.5** and **S3** showed a continuous decrease of their apparent viscosity during the time interval in which the higher shear rate was applied. The other samples kept a constant viscosity during the stepwise corresponding to 10 s^{-1}. The sudden decrease of the applied shear rate to 0.2 s^{-1} caused the structure regeneration of all samples leading to the increase of their apparent viscosity. The regeneration manner of the structure and its recovery degree after the decrease of the shear rate, depended on the amount of salicylaldehyde of the hydrogel samples. Generally, a material which has a recovery degree in the third stepwise reported to the first ones higher than 70% is considered to have a good thixotropic recovery [Patel, & Dewettinck, 2015]. Thereby, **S1.5** and **S2** hydrogels which have recovered 82.2 % and 74.8 %, respectively from their initial viscosity in about 20 minutes proved a good thixotropic behaviour. The samples obtained with a lower amount of crosslinker (**S2.5-S3.5**) revealed an increase of the apparent viscosity over the equilibrium value at the sudden change of the shear rate from 10 s^{-1} to 0.2 s^{-1}. After that, the regenerated structures reached the equilibrium viscosity in around 1 hour.

Swelling behaviour

The swelling behaviour is an important characteristic of the hydrogels which recommend them for applications as absorbents, drug delivery or filtration/separation systems, soil conditioners, and so on [Porter, Stewart, Reed, & Morton, 2007]. As different biological fluids have different pH, the swelling of the xerogel samples was monitored in three swelling media: water at neutral pH; phosphate buffer solution (PBS) with a pH of 7.4, close to the one of tissues and acetate buffer solution with a pH of 4.2, close to the one of vagina. In all these media, the xerogels samples rehydrated forming the initial hydrogel. As can be seen in Figure 7, the swelling strongly depended on the pH of the media and the crosslinking density. All the xerogel samples swelled very fast, in about 1 minute, reminiscent of superporous hydrogels of

third generation used as superabsorbents or in gastrointestinal devices as well as in pharmaceutical and biomedical applications [Omidian, Rocca & Park, 2005; Ahmed, Chatterjee, Chauhan, Jaimini & Varshney, 2014]. As the crosslinking density decreased the swelling ratio increased, in a close correlation with the morphology change from interconnected pores (**S1**) to a microfibrous network (**S3**) with an increased flexibility. The higher swelling capacity of the sample **S3** with lower crosslinking density was attributed to the higher flexibility of the free chitosan chains, behaviour also observed for other chitosan based superporous hydrogels [Gupta, & Shivakumar, 2010].

In the acidic media, the hydrogels were the least stable, the **S3** and **S2.5** hydrogels completely dissolved in about 10 minutes; **S2** and **S1.5** in three days and **S1** in five days. The low swelling ratio measured in acidic media was the most probably the result of the competition between the swelling and dissolving processes because the acidic media favoured the shifting of the imination equilibrium to the reagents.

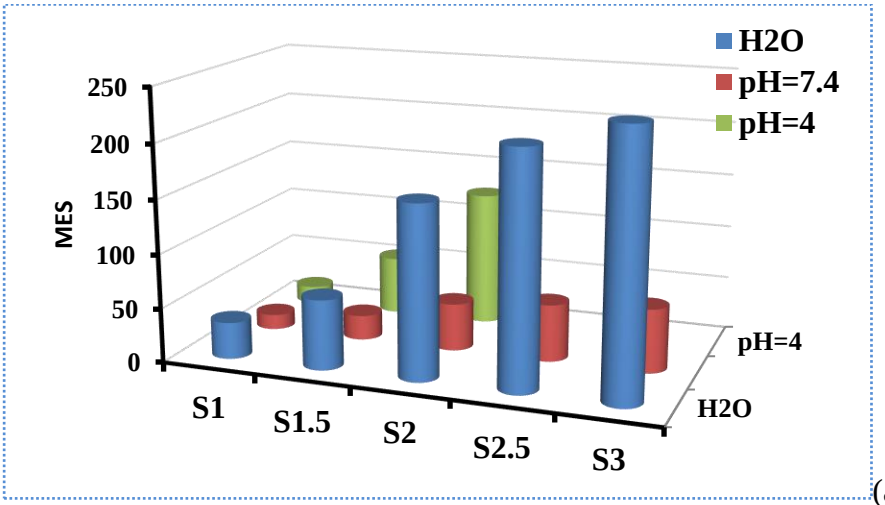

(a)

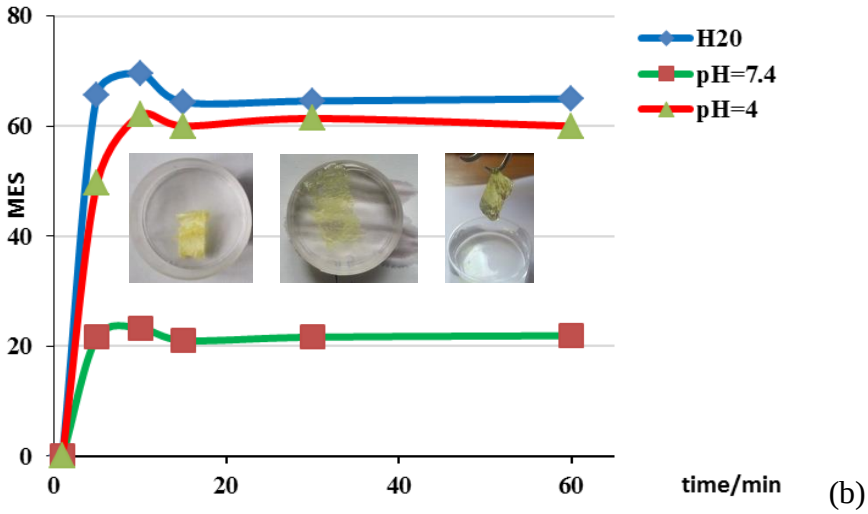

(b)

Figure 7. Mass equilibrium swelling (MES) in different pH media of the (a) studied hydrogels; (b) **S1.5** measured at different times

The mass equilibrium swelling (MES) of the hydrogels increased progressively from 14 to 53 – in basic pH media, and from 34 to 240 – in water, respectively, as the crosslinking degree diminished. Remarkable, the swollen hydrogels were stable even after 3 months. Their analysis by FTIR spectroscopy, revealed similar spectra with those of the initial xerogels, showing that imine linkage was not affected in water or basic media (Figure 4s). As the model compound proved no stability in aqueous media (Figure 5s) the stability of the imine linkages into hydrogels can be attributed to the forming of hydrophobic clusters which protect them against water.

Macroscopic self-healing properties of the hydrogels

As the process of the hydrogel gelling was realized based on reversible covalent imine linkages, it was expected to present self-healing properties. Indeed, cutting a hydrogel in two pieces and connecting them back, they adhere one to each other at room temperature (25 ^{o}C) into one integral piece in less than 1 hour (Figure 6s a,b). Moreover, crushing a hydrogel from

a vial in small pieces and heating the vial at the human body temperature (37 ^{o}C), the small pieces adhere one to each other reshaping the hydrogel (Figure 6s c, d).

CONCLUSIONS

In summary, we synthesised hydrogels based on two naturally derived compounds chitosan and salicylaldehyde by a novel, simple and green method based on dynamic covalent chemistry. The unusual crosslinking of chitosan with the monoaldehyde has been reached due to the supramolecular assistance of the molecular synthesis at three dynamic levels consisting in (i) self-assembly, (ii) self-organization, and (iii) segregation processes. Thus, the self-assembling of chitosan with salicylaldehyde took place *via* reversible imine bond further stabilized by an "imine clip" effect. The newly formed rigid imine units self-organized together in hydrophobic associations favoured by the motional processes of the salicylaldehyde between amino groups by reversible covalent imine formation. The forming of the hydrophobic associations facilitated a hydrophilic/hydrophobic segregation to give ordered clusters which acted as net nodes linking the chitosan chains. Rheological measurements were established that the minimum ratio of the amine to aldehyde functional groups necessary for chitosan crosslinking is 3.2. The supramolecular arrangement of the salicyl-imine-chitosan hydrogels strongly influenced their properties. The hydrogels were elastic, exhibited thixotropic behaviour and were thermosensitive – important features for bio-related applications. They completely rehydrated in water, PBS and acetate buffer and swelled very fast reaching MES values of 240. In acetate buffer, the dissolution time of the hydrogels depended by the crosslinking degree, varying between 10 minutes and 5 days while in water and PBS buffer, the hydrogels kept their integrity even after few months. The hydrogels exhibited luminescence and self-healing ability at room temperature and body temperature as well.

The paper reports a new chitosan based hydrogel with attractive properties for bio-related applications, but more important it brings into attention a new concept of chitosan crosslinking with monoaldehydes (which are abundant in nature and have own valuable therapeutic properties) which open large perspectives for the developing of the hydrogels domain.

ACKNOWLEDGEMENTS

The research leading to these results has received funding from the Romanian National Authority for Scientific Research, MEN – UEFISCDI grant, project number PN-II-RU-TE-2014-4-2314 and from European Union's Horizon 2020 research and innovation program under grant agreement no: 667387.

REFERENCES

Adams, T.B., Cohen, S.M., Doull, J., Feron, V.J., Goodman, J.I., Marnett, L.J., Munro, I.C., Portoghese, P.S., Smith, R.L., Waddell, W.J. & Wagner B.M. (2005). The FEMA GRAS assessment of hydroxy- and alkoxy-substituted benzyl derivatives used as flavor ingredients. *Food and Chemical Toxicology***,** 43, 1241–1271.

Ahmed, E. M. (2015**)**. Hydrogel: Preparation, characterization, and applications: A review. *Journal of Advanced Research*, *6*, 105–121.

Ahmed, J. A., Chatterjee, A., Chauhan, B. S., Jaimini, M. & Varshney, H. M. A (2014). Conceptual Overview on Superporous Hydrogels. *International Journal of Pharmaceutical Science Review* & *Research*, *25*, 166–73.

Ailincai, D., Marin, L., Morariu, S., Mares, M., Bostanaru, A. C., Pinteala, M., Simionescu B.C. & Barboiu, M. Dual crosslinked iminoboronate-chitosan hydrogels with strong antifungal

activity against Candida planktonic yeasts and biofilms. (2016). *Carbohydrate Polymers*, *152*, 306–316.

Barcan, G. A., Zhang X. & Waymouth, R. M. (2015). Structurally Dynamic Hydrogels Derived from 1,2-Dithiolanes. *Journal of American Chemical Society*, *137*, 5650–5653.

Baron, M. (2001). Definitions of Basic Terms Relating to Low-Nolar-Mass and Polymer Liquid Crystals. *Pure and Applied Chemistry*, *73*, 845–895.

Beauchamp, R. O., St Clair, M. B., Fennell, T. R., Clarke D. O., Morgan, K. T. (1992). A Critical Review of the Toxicology of Glutaraldehyde. *Critical Reviews of Toxicology*, *22*, 143–174.

Bejan, A., Shova, S., Damaceanu, M. D., Simionescu, B. C., Marin, L. (2016). Structure-Directed Functional Properties of Phenothiazine Brominated Dyes: Morphology and Photophysical and Electrochemical Properties, *Crystal Growth and Design*, *16*, 3716–3730.

Bercea, M., Bibire, E.-L., Morariu, S., Teodorescu M. & Carja, G. (2015). Effect of Cryogenic Treatment on the Rheological Properties of Chitosan/Poly(vinyl alcohol) Hydrogels. *European Polymer Journal*, *70*, 147–156.

Berger, J., Reist, M., Mayer, J. M., Felt, O., Peppas, N. A. & Gurny, R. (2004). Structure and Interactions in Covalently and Ionically Crosslinked Chitosan Hydrogels for Biomedical Applications. *European Journal of Pharmaceutics and Biopharmaceutics*, *57*, 19–34.

Bhattarai, N., Gunn, J. & Zhang, M. (2010). Chitosan-based hydrogels for controlled, localized drug delivery. *Advanced Drug Delivery Reviews*, *62*, 83–99.

Brooks W. L. A. & Sumerlin, B. S. (2016). Synthesis and Applications of Boronic Acid-Containing Polymers: From Materials to Medicine. *Chemical Reviews*, *116*, 1375–1397.

Caló, E. & Khutoryanskiy, V. V. (2015)**.** Biomedical applications of hydrogels: A review of patents and commercial products. *European Polymer Journal*, *65*, 252–267.

Casuso, P., Odriozola, I., Pérez-San Vicente A., Loinaz, I., Cabañero, G., Grande H. J. & Dupin, D. (2015). Injectable and Self-Healing Dynamic Hydrogels Based on Metal(I)-Thiolate/Disulfide Exchange as Biomaterials with Tunable Mechanical Properties. *Biomacromolecules*, *16*, 3552–3561.

Casuso, P., Perez-San Vicente, A., Iribar, H., Gutierrez-Rivera, A., Izeta, A., Loinaz, I., Cabanero, G., Grande, H-J., Odriozola, I. & Dupin, D. (2014**).** Aurophilically cross-linked "dynamic" hydrogels mimicking healthy synovial fluid properties. *Chemical Communications*, *50*, 15199–15201.

Chambon, F. & Winter, H.H. (1987). Linear viscoelasticity at the gel point of a crosslinking PDMS with imbalanced stoichiometry. *Journal of Rheology, 31*, 683–697.

Clima, L., Peptanariu D., Pinteala, M., Salic A. & Barboiu, M. (2015). Dynavectors: Dynamic Constitutional Vectors for Adaptive DNA Transfection. *Chemical Communications, 51*, 17529–17531.

Costa Pessoa, J., Tomaz, I. & Henriques, R.T. (2003). Preparation and characterisation of vanadium complexes derived from salicylaldehyde or pyridoxal and sugar derivatives. *Inorganica Chimica Acta*, *356*, 121–132.

CrysAlis RED, Oxford Diffraction Ltd., Version 1.171.36.32, 2003.

da Silva, C. M., da Silva, D. L., Modolo, L. V., Alves, R. B., de Resende, M. A., Martins, C. V. B., & de Fátima, Â. (2011). Schiff bases: A short review of their antimicrobial activities. *Journal of Advanced Research*, *2*, 1–8.

de Araújo, E.L., Barbosa, H.F.G., Dockal, E. R. & Cavalheiro, E.T.G. (2017). Synthesis, characterization and biological activity of Cu(II), Ni(II) and Zn(II) complexes of biopolymeric Schiff bases of salicylaldehydes and chitosan. *International Journal of Biological Macromolecules*, *95*,168–176.

De Vries, A. (1970). X-ray Photographic Studies of Liquid Crystals I. A Cybotactic Nematic Phase. *Molecular Crystal and Liquid Crystal*, *10*, 219–236.

Delmar, K. & Bianco-Peled, H. (2016). Composite chitosan hydrogels for extended release of hydrophobic drugs. C*arbohydrate Polymers*, *136*, 570–580.

Deng, G., Tang, C., Li, F., Jiang H. & Chen, Y. (2010). Covalent Cross-Linked Polymer Gels with Reversible Sol-Gel Transition and Self-Healing Properties. *Macromolecules*, *43*, 1191–1194.

Deng, P., Fei, J., Feng, Y. (2011). Sensitive voltammetric determination of tryptophan using an acetylene black paste electrode modified with a Schiff's base derivative of chitosan, *Analyst*, *136*, 5211–5217.

Destri, S., Khotina, I. A. & Porzio, W. (1991). 3-Hexyl Tetra-Substituted Sesquithienylene-Phenylene Polyazomethines with High Molecular Weight. Mechanistic Considerations. *Macromolecules*, *31*, 1079–1086.

Dinu, M. V., Ozmen, M. M., Dragan, E. Z. & Okay O. (2007). Freezing as a Path to Build Macroporous Structures: Superfast Responsive Polyacrylamide Hydrogels. *Polymer*, *48*, 195–204.

Dolomanov, O. V., Bourhis, L. J., Gildea, R. J., Howard, J. A. K. & Puschmann, H. (2009). Olex2: A complete structure solution, refinement and analysis program. *Journal of Applied Crystallography*, *42*, 339–341.

dos Santos, J. E., Dockal, E. R. & Cavalheiro, E´. T. G. (2005). Synthesis and characterization of Schiff bases from chitosan and salicylaldehyde derivatives. *Carbohydrate Polymers*, *60*, 277–282.

Filarowski, A. (2005). Intramolecular hydrogen bonding in *o*-hydroxyaryl Schiff bases. *Journal of Physical Organic Chemistry*, *18*, 686–698.

Fisher, H. F. & Viswanathan, T. S. (1984). Carbonyl oxygen exchange evidence of imine formation in the glutamate dehydrogenase reaction and identification of the "occult role" of NADPH. *Proceedings of the National Academy of Science USA*, *81*, 2747–2751.

Garrick, L. M., Gniecko, K., Hoke, J. E., Alnakeeb, A., Ponka P. & Garrik, M. D. (1991). Ferric-Salicylaldehyde Isonicotinoyl Hydrazone, a Synthetic Iron Chelate, Alleviates Defective Iron Utilization by Reticulocytes of the Belgrade Rat. *Journal of Cellular Physiology*, *146*, 460–465.

Giri, T. K., Thakur, A., Alexander, A., Ajazuddin, Badwaik, H. & Tripathi, D. K. (2012). Modified chitosan hydrogels as drug delivery and tissue engineering systems: present status and applications, *Acta Pharmaceutica Sinica B*, *2*, 439–449.

Gupta, N.V. & Shivakumar, H.G. (2010). Preparation and characterization of superporous hydrogels as gastroretentive drug delivery system for rosiglitazone maleate. *Daru*, *18*, 200–210.

Kim, J. H., Campbell, B. C., Mahoney, N., Chan, K. L. & Molyneux, R. J. (2011). Chemosensitization of Aflatoxigenic Fungi to Antimycin A and Strobilurin Using Salicylaldehyde, a Volatile Natural Compound Targeting Cellular Antioxidation System. *Mycopathologia*, *171*, 291–298.

Kovaricek, P. & Lehn, J. M. (2012). Merging constitutional and motional covalent dynamics in reversible imine formation and exchange processes. *Journal of American Chemical Society*, *134*, 9446–9455.

Kumirska, J., Czerwicka, M., Kaczyński, Z., Bychowska, A., Brzozowski, K. Thöming, J. & Stepnowski, P. (2010). Application of Spectroscopic Methods for Structural Analysis of Chitin and Chitosan. *Marine Drugs*, *8*, 1567–1636.

Lambert J. & Muir, T.A. (1973). *Practical chemistry*, 3rd. Ed. Heineman, London

Liu Y. & Lim, Z. T. (2013). A Dynamic Route to Structure and Function: Recent Advances in Imine-Based Organic Nanostructured Materials. *Austrian Journal of Chemistry*, *66*, 9–22.

Ma, Q. & Wang, Q. (2015). Lanthanide induced formation of novel luminescent alginate hydrogels and detection features,*Carbohydrate Polymers*, *133*, 19–23.

Marin, L., Ailincai, D., Cahn, M., Stan, D., Constantinescu, C. A., Ursu, L., Doroftei, F., Pinteala, M., Simionescu B. C. & Barboiu, M. (2016). Dynameric Frameworks for DNA Transfection. *ACS Biomaterials Science and Engineering*, *2*, 104–111.

Marin, L., Ailincai, D., Mares, M., Paslaru, E., Cristea, M., Nica V. & Simionescu, B. C. (2015). Imino-Chitosan Biopolymeric Films. Obtaining, Self-assembling, Surface and Antimicrobial Properties. *Carbohydrate Polymers*, *117*, 762–770.

Marin, L., Morariu, S., Popescu, M. C., Nicolescu, A., Zgardan, C., Simionescu B. C. & Barboiu, M. (2014). Out-of-Water Constitutional Self-Organization of Chitosan–Cinnamaldehyde Dynagels. *Chemistry- A European Journal*, *20*, 4814–4821.

Marin, L., Simionescu B. C. & Barboiu, M. (2012). Imino-chitosan biodynamers. *Chemical Communications*, *48*, 8778–8780.

Marin, L., van der Lee, A., Shova, S., Arvinte, A. & Barboiu, M. (2015). Molecular amorphous glasses toward large azomethine crystals with aggregation-induced emission. *New Journal of Chemistry*, *39*, 6404–6420.

Menaka, R. & Subhashini, S. (2016). Chitosan Schiff base as eco-friendly inhibitor for mild steel corrosion in 1M HCl, *Journal of Adhesion Science and Technology*, 30, 1622–1640.

Mikhailov, S. N., Zakharova, A. N., Drenichev, M. S., Ershov, A. V., Kasatkina, M. A., Vladimirov, L. V., Novikov, V. V. & Kildeeva, N. R. (2016). Crosslinking of Chitosan with Dialdehyde Derivatives of Nucleosides and Nucleotides. Mechanism and Comparison with Glutaraldehyde. *Nucleosides, Nucleotides and Nucleic Acids*, *35*, 114–129.

Morariu, S., Bercea, M. & Brunchi, C.-E. (2015). Effect of Cryogenic Treatment on the Rheological Properties of Chitosan/Poly(vinyl alcohol) Hydrogels. *Industrial and Engineering Chemical Research*, *54*, 11475–11482.

Nasr, G., Petit, E., Vullo, D., Winum, J.-Y., Supuran C. T. & Barboiu, M. (2009). Carbonic Anhydrase-Encoded Dynamic Constitutional Libraries: Toward the Discovery of Isozyme-Specific Inhibitors. *Journal of Medicinal Chemistry*, *52*, 4853–4859.

Nawrotek, K., Tylman, M., Rudnicka, K., Balcerzak, J. & Kamiński, K. (2016). Chitosan-based hydrogel implants enriched with calcium ions intended for peripheral nervous tissue regeneration. *Carbohydrate Polymers*, *136*, 764–771.

Nguyen, T. D., Nguyen, Q. V., Ho, H. T. & Ngo, D. B. T. (2011). Investigation of synthetic reaction of azomethines from glucosamine and substituted benzaldehyde. *Proceedings of the 15th International Electronic Conference on Synthetic Organic Chemistry*, Sciforum Electronic Conference series, *15*, a024.

Omidian, H., Rocca, J. G. & Park, K. (2005). Advances in superporous hydrogels. *Journal of Controlled Release*, *102*, 3–12.

Patel, A.R. & Dewettinck, K. (2015). Comparative evaluation of structured oil systems: Shellac oleogel, HPMC oleogel, and HIPE gel. *European Journal of Lipid Science and Technology*, *117*, 1772–1781.

Perez, D. M. & Karnik, S. S. (2005). Multiple Signalling States of G-Protein-Coupled Receptors. *Pharmacological Reviews, 57,* 147–161.

Porter, T. L., Stewart, R., Reed, J. & Morton, K. (2007). Models of Hydrogel Swelling with Applications to Hydration Sensing. *Sensors*, *7*, 1980–1991.

Qin, W., Long, S., Panunzio M. & Biondi, S. (2013). Schiff Bases: A Short Survey on an Evergreen Chemistry Tool. *Molecules*, 18, 12264–12289.

Ramstrom, O., Lohmann, S., Bunyapaiboonsri, T. & Lehn, J. M. (2004). Dynamic Combinatorial Carbohydrate Libraries: Probing the Binding Site of the Concanavalin A Lectin. *Chemistry - A European Journal*, *10*, 1711–1715.

Roy, N., Bruchmannb B. & Lehn, J. M. (2015). Dynamers: Dynamic Polymers as Self-Healing Materials. *Chemical Society Reviews*, *44*, 3786–3807.

Sagiomo, V. & Luning, U. (2009). On the formation of imines in water - a comparison. *Tetrahedron Letters*, *50*, 4663–4665.

Salicylaldehyde (1979). *Food and Cosmetics Toxicology*, *17*, 903–905.

Sheldrick, G. M. (2008**)**. A short history of Shelx. *Acta* Crysttalographica, *A64*, 112–122.

Shen, X., Shamshina, J. L., Berton, P., Gurau G. & Rogers, R.D. (2016)**.** Hydrogels based on cellulose and chitin: fabrication, properties, and applications. *Green Chemestry***,** *18***,** 53–75.

Sreenivasachary, N. & Lehn, J. M. (2005). Gelation-Driven Component Selection in the Generation of Constitutional Dynamic Hydrogels Based on Guanine-Quartet Formation. *Proceedings of the National Academy of Science USA*, *102*, 5938–5943.

Sun, Y., Lin, L., Deng, H., Li, J., He, B., Sun, R. & Ouyang, P. (2008). Structural changes of bamboo cellulose in formic acid. *BioResources*, *3*, 297–315.

Turin-Moleavin, I. A., Doroftei, F., Coroaba, A., Peptanariu, D., Pinteala, M., Salic A. & Barboiu, M. (2015). Dynamic constitutional frameworks (DCFs) as nanovectors for cellular delivery of DNA. *Organic Biomolecular Chemistry*, *13*, 9005–9011.

Wang, Q., Mynar, J. L., Yoshida, M., Lee, E., Okura, K., Kinbara, K. & Aida, T. (2010). High-water-content mouldable hydrogels by mixing clay and a dendritic molecular binder. *Nature*, *463*, 339–343.

Zaltariov, M. F., Vlad, A., Cazacu, M., Avadanei, M., Vornicu, N., Balan, M. & Shova, S. (2015). Silicon-containing bis-azomethines: Synthesis, structural characterization, evaluation of the photophysical properties and biological activity. *Spectrochimica Acta A*, *138*, 38–48.

Zhang, S. & Chen, Y. (2015). Nanofabrication and coloration study of artificial *Morpho* butterfly wings with aligned lamellae layers. *Scientific Reports*, *5*, Article number: 16637.

Zhang, Y. & Barboiu, M. (2016). Constitutional Dynamic Materials - Toward Natural Selection of Function. *Chemical Reviews*, *116*, 809–834.

Zhang, Y., Tao, L., Li, S. & Wei, Y. (2011). Synthesis of Multiresponsive and Dynamic Chitosan-Based Hydrogels for Controlled Release of Bioactive Molecules. *Biomacromolecules*, *12*, 2894–2901.

TOC graphic